

Liquid-Crystalline Hybrid Materials Based on [60]Fullerene and Bent-Core Structures**

Jorge Vergara, Joaquín Barberá, José Luis Serrano, M. Blanca Ros,* Nerea Sebastián, Rosario de la Fuente, David O. López, Gustavo Fernández, Luis Sánchez, and Nazario Martín

The incorporation of the [60]fullerene moiety into molecular materials is currently a common strategy for the design of functional materials, particularly in the field of molecular electronics.^[1] The appeal of this strategy is due to the unique properties of the [60]fullerene structure,^[2] which can be chemically manipulated for incorporation into suitable molecular structures.^[2h,i,3] Moreover, the design and development of new functional C₆₀ derivatives in combination with other organic structures in a cost-effective way is a challenging target for fullerene and supramolecular chemists.^[4]

With regard to this aim, liquid crystals are excellent candidates for organizing fullerenes within supramolecular ordered structures, and various morphologies of C₆₀-containing liquid crystals, such as nematic, cholesteric, smectic, or columnar phases, have been reported in the last decade.^[4d,5-7] Outstanding results have been achieved with liquid-crystalline fullerodendrimers with a low C₆₀ content.^[4d,7] In contrast, studies on C₆₀-based liquid-crystal materials with a high fullerene content and with simpler molecular structures are scarce,^[5,8] possibly because the appropriate combination of

C₆₀ units with other organic functional structures to attain mesomorphism is not an easy task.

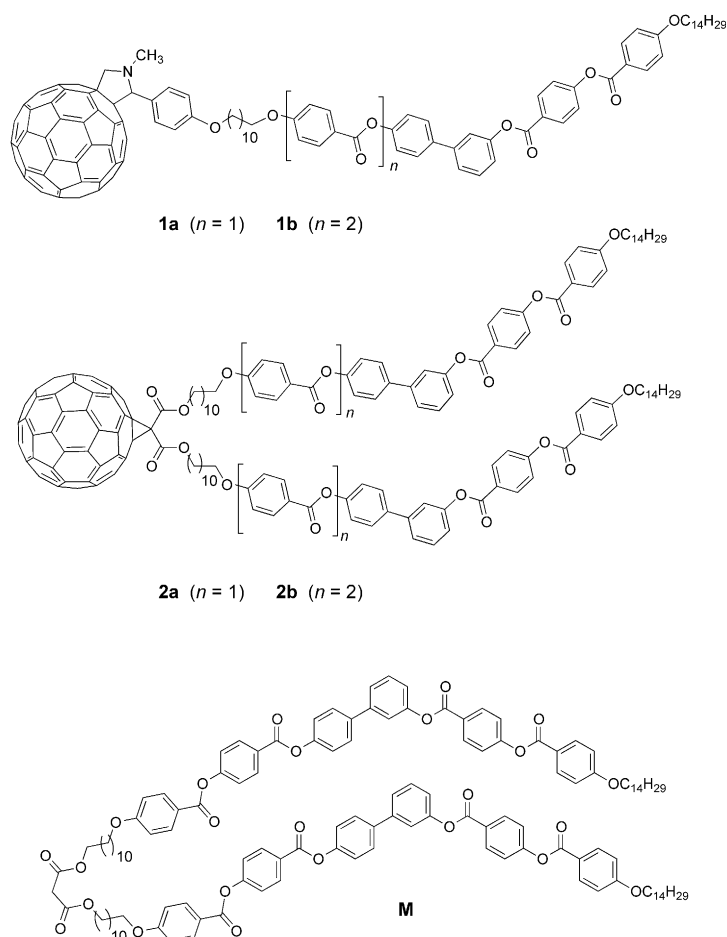
Herein, we report the synthesis and characterization of a new class of nondendritic hybrid C₆₀-containing bent-shaped molecules. The aim of this work was to take advantage of the unique properties derived from the compact packing of bent-core structures. In 1996 this class of kinked structure was found to form bent-core liquid crystals, which is a less common and intriguing type of mesomorphism.^[9] In contrast to calamitic mesophases, bent-shaped molecules, through dense arrangements that hinder the molecular rotation, lead to strong polar order within either layers or columns, in many cases producing supramolecular chirality with achiral molecules. The molecules can often be switched in these mesophases by external stimuli, and they have afforded exceptionally good macroscopic polarization values and piezoelectric, flexoelectric, and nonlinear optical responses.^[10] We report herein four C₆₀-based bent-core compounds (Scheme 1). Compounds **1a** and **1b** are fulleropyrrolidine monoadducts with a 1:1 C₆₀/promesogenic-core ratio. In contrast, a 1:2 ratio is present in the case of the methanofullerene derivatives **2a** and **2b**. In both types of molecules, two rigid cores of different lengths have been used to promote the liquid-crystal order.

Fullerene derivatives **1a**, **1b**, **2a**, and **2b** were synthesized by the synthetic routes depicted in Schemes S1, S2, and S3 (see the Supporting Information). Fulleropyrrolidines **1a** and **1b** were prepared from a C₆₀-containing acid. This intermediate was synthesized by the [3+2] dipolar cycloaddition of C₆₀ with a suitably functionalized azomethine ylide, which was generated in situ from a substituted benzaldehyde and *N*-methylglycine, followed by hydrogenolysis.^[11] The esterification of the C₆₀-containing acid with a 3,4'-biphenyl-based biphenol,^[12] with 4-(*N,N*-dimethylamino)pyridinium-4-toluenesulfonate (DPTS)/dicyclohexylcarbodiimide (DCC), gave the bent-core fulleropyrrolidines **1a** and **1b**. Two alternative synthetic routes were assessed to prepare the methano[60]fullerene monoadducts **2a** and **2b**. Both synthetic approaches were based on the Bingel reaction to join the [60]fullerene to the malonate structures.^[13] Route 1 involved esterification of the C₆₀ diacid with the corresponding 3,4'-biphenyl derivatives, also using DPTS/DCC, to give compounds **2a** and **2b**. A second synthetic pathway (Route 2) was also used for compound **2b**, but this gave lower yields than Route 1 and the preparation of a bent-core malonate (compound **M**; see Scheme 1 and Scheme S3 in the Supporting Information) was required prior to the addition to C₆₀ in the final synthetic step.

[*] Dr. J. Vergara, Dr. J. Barberá, Prof. M. B. Ros
 Dpto. Química Orgánica
 Instituto de Ciencia de Materiales de Aragón (I.C.M.A.)
 Facultad de Ciencias, Universidad de Zaragoza
 C.S.I.C., 50009-Zaragoza (Spain)
 E-mail: bros@unizar.es
 Prof. J. L. Serrano
 Dpto. Química Orgánica, Instituto de Nanociencia de Aragón
 Universidad de Zaragoza, 50009-Zaragoza (Spain)
 N. Sebastián, Prof. R. de la Fuente
 Dpto. Física Aplicada II, Facultad de Ciencia y Tecnología
 Universidad del País Vasco, Apdo 644, 48080-Bilbao (Spain)
 Dr. D. O. López
 Grup de les Propietats Físiques dels Materials (GRPFM)
 Departament de Física i Enginyeria Nuclear
 E.T.S.E.I.B. Universitat Politècnica de Catalunya
 Diagonal, 647, 08028 Barcelona (Spain)
 Dr. G. Fernández, Dr. L. Sánchez, Prof. N. Martín
 Departamento de Química Orgánica
 Facultad de Ciencias Químicas
 Ciudad Universitaria s/n, 28040 Madrid (Spain)

[**] This research is supported by the MICINN-FEDER of Spain-UE MAT2009-14636-CO3, CT2008-00795, CSD2007-00010, the Aragón (E04), Basque (GI/IT-449-10), and Madrid (S2009/PPQ-1533) governments. We are also grateful to BSCH-UZ and the Aragon government (J.V.) and Basque Country (N.S.) for fellowship grants and Dr. B. Villacampa from ICMA for the SHG measurements.

Supporting information for this article is available on the WWW under <http://dx.doi.org/10.1002/anie.201104866>.



Scheme 1. Chemical structures of the C_{60} -based bent-core compounds prepared and the intermediate malonate **M**.

All new compounds were characterized by MALDI-TOF mass spectrometry and ^1H NMR, ^{13}C NMR, and FTIR spectroscopy. The presence of C_{60} monoadducts was also confirmed by UV/Vis spectroscopy from the observation of the characteristic absorption peaks at around 430 nm. Thermogravimetric analysis (TGA) studies showed that these compounds exhibit weight loss above 320°C (see the Supporting Information).

The redox features of the C_{60} derivatives reported here were investigated by cyclic voltammetry (CV) in ODCB/ CH_3CN 4:1 (ODCB = *o*-dichlorobenzene) at room temperature using a glassy carbon working electrode, standard Ag/AgCl as the reference electrode, and tetrabutylammonium perchlorate (0.1M) as the supporting electrolyte. The voltammograms of all the fullerene derivatives exhibit three quasi-reversible one-electron reduction waves at potentials of -0.86 , -1.29 , and -1.79 V in the case of **1a** and **1b**, and -0.78 , -1.18 , and -1.66 V for methanofullerene monoadducts **2a** and **2b** (see the Supporting Information). These values are slightly anodically shifted in comparison to pure [60]fullerene because of saturation of one of the double bonds of the C_{60} cage with the subsequent raising of the corresponding LUMO level (see Ref. [14]).

The thermal and liquid-crystalline properties of the compounds were investigated by polarized optical microsc-

py (POM), X-ray diffraction (XRD) at variable temperature, and differential scanning calorimetry (DSC and MDSC).^[15] Thus, the phase-transition enthalpy and specific-heat (C_p) changes were analyzed. The phase-transition temperatures and enthalpies are reported in Table 1.

In spite of their dark brown color, optical textures of the annealed samples could be observed and these showed very small defects that exhibit birefringence and confirmed the fluid nature of **1b**, **2a**, and **2b** at a range of temperatures (Figure 1).

Differential scanning calorimetry revealed the unique thermal behavior of these [60]fullerene compounds as well as slow kinetic transitions. Upon heating, endothermic peaks corresponding to the crystalline-to-mesomorphic and mesomorphic-to-isotropic phase transitions were detected for **1b**, **2a**, and **2b**. However, on cooling of the isotropic liquid, different evolutions were observed. Concerning transitions from the liquid phase, significant thermal hysteresis was shown by **1b** and **2a** on cooling and this prevented the formation of a stable mesophase. However, this was not the case for **2b**, which exhibited an enantiotropic mesophase (Figure 2). Interestingly, successive heating and cooling processes revealed repetitive thermal behavior for these hybrid compounds. Moreover, C_p studies by MDSC at a rate of 1°Cmin^{-1} revealed further changes below 60°C for all the [60]fullerene compounds and this is consistent with a glass transition (see the Supporting Information).

To analyze the supramolecular organization of these mesomorphic molecules, powder XRD studies

Table 1: Phase-transition behavior of the [60]fullerene bent-core compounds and malonate **M**.

Compound	Phase transitions ^[a-c]
1a	Cr 62 (11) I I 49 g
1b	Cr-SmCP 183 (25) ^[d] I I 110 (20) Cr
2a	Cr 102 (20) SmCP 134 (14) I I 100 (28) Cr
2b	g 57 SmCP 160 (28) I I 141 (27) SmCP 54 g
M	Cr-Col 137 (62) ^[e] I I 134 Col 81 Cr

[a] Transition temperature ($^\circ\text{C}$) at the slope of the peak and [b] enthalpies (kJ mol^{-1} , in parenthesis), determined on the second scans by DSC ($10^\circ\text{C min}^{-1}$). [c] Cr = crystalline, g = glass, I = isotropic liquid, SmCP = smectic C polar mesophase, Col = columnar mesophase. [d] From a broad peak and combined enthalpies. [e] Associated with a very slow kinetic of transition. A similar enthalpy value has been obtained from specific-heat data in MDSC measurements at 1 Kmin^{-1} . On cooling, the observed peak does not correspond to the full transformation to the stable mesophase.

were performed (Table 2). The XRD patterns recorded at high temperatures for compounds **1b**, **2a**, and **2b** show a broad halo in the high-angle region centered at $4.5\text{--}4.6\text{ \AA}$.

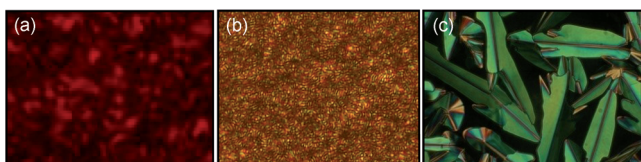


Figure 1. Microphotographs of the textures corresponding to the mesophases of the compounds: a) **1b** (178 °C, SmCP), b) **2b** (134 °C, SmCP), and c) compound **M** (132 °C, Col).^[19]

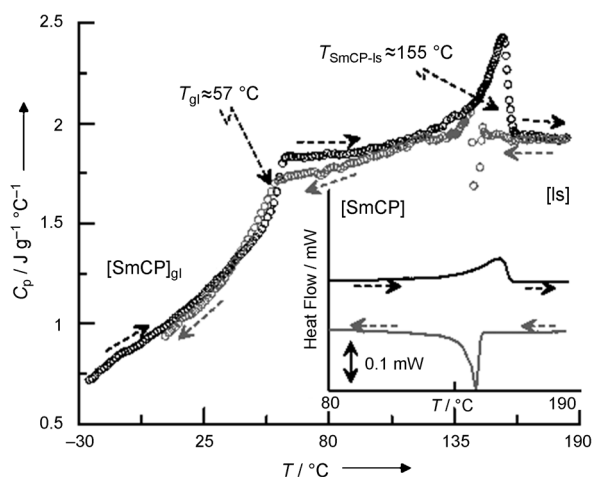


Figure 2. Specific-heat data for compound **2b** on heating (black symbols) and on cooling (gray symbols). The inset shows typical DSC scans on heating (black curve) and on cooling (gray curve) at 1 °C min⁻¹. gl = glassy, Is = isotropic liquid phase.

This halo is assigned to the melting of the terminal chains and it confirms the liquid-crystalline nature of the phases. In addition, up to three sharp peaks in a 1:3:4 ratio were observed at small angles, which can be respectively indexed as

Table 2: X-ray diffraction data for the [60]fullerene bent-core compounds.

Cmpd.	T [°C]	Measured spacing [Å]	Miller index	Layer thickness (d) [Å]
1b	175 ^[a]	97.0	001	98.0
		32.9	003	
		24.5	004	
		4.5 ^[d]		
2a	RT ^[b]	31.3	003	94
		9.0 ^[d]		
		4.5 ^[d]		
		87.5	001	
29.4	003			
9.0 ^[d]				
4.6 ^[d]				
2b	140 ^[c]	88.6	001	89.1
		29.6	003	
		22.5	004	
		9.0 ^[d]		
2b	RT ^[c]	4.6 ^[d]		87.5
		87.3	001	
		29.2	003	
		9.0 ^[d]		
		4.6 ^[d]		

[a] Heating process. [b] After rapid cooling to prevent crystallization. [c] Cooling process. [d] Diffuse maximum.

the (001), (003), and (004) reflections of a lamellar structure. For **2a** a room temperature pattern could also be recorded by freezing the mesophase (by rapid cooling from 126 °C to avoid crystallization). For **2b** a room temperature pattern was recorded for the glassy mesophase. The layer thicknesses, measured from the small-angle reflections, are shown in Table 2. This kind of pattern is unambiguously consistent with a lamellar bent-core mesophase-like order.

Furthermore, the diffraction patterns of the two methane adducts, **2a** and **2b**, also contain a middle-angle diffuse signal at about 9 Å, which has been reported for other C₆₀-containing liquid crystals^[5d,f,6d,16] and has been attributed to interactions between the fullerene units. This finding points to a more-organized packing of the molecules for the mesophase of these two compounds, with close contact between the C₆₀ units compared to the mesophase of **1b**. These features, the measured layer spacing, as well as the POM observations, and mesomorphic-to-isotropic phase-transition enthalpies are consistent with a bilayer assembly of tilted bent-shaped molecules (tentatively assigned as a smectic C polar (SmCP) mesophase).^[17] In the mesophase each molecule is folded with the two bent-core units oriented in the same direction (Figure 3), a situation consistent with the reported simulation studies on C₆₀-calamitic and C₆₀-discotic dimesogens.^[8c] The

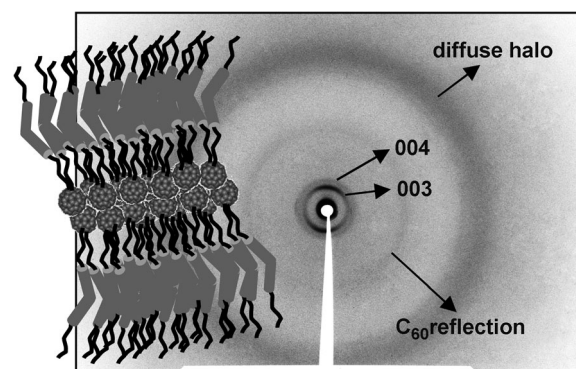


Figure 3. Proposed molecular packing in the lamellar mesophase and the glassy mesophase of compound **2b** and X-ray diffraction patterns at room temperature. The 001 reflection is partially hidden under the beam stop, but is clearly detected in the small-angle XRD experiments.

fullerenes occupy the central area of the bilayer in a head-to-head arrangement and the hydrocarbon chains form an aliphatic region between neighboring layers.

This kind of organization allows for a reasonable fit between the cross-sectional areas of the C₆₀ and the mesogenic units,^[5b,7b] and ensures efficient space filling because the fullerene cross-section accommodates two mesogenic units.^[18]

Therefore, practically no interdigitation is expected between the C₆₀ heads, a situation which is in reasonable agreement with the XRD results reported for alkylated fullerenes.^[8b] The differences observed in the measured layer spacing can be accounted for by changes in the tilt angle of the molecule. The mesophase of **1b** also probably has a bilayer structure, based on the measured layer spacing. However, in this case a dramatic mismatch must take place between the

cross-sections of fullerene and the single mesogenic unit, and this may explain the difficulty for the molecules of this compound to organize themselves in the cooling process from the isotropic liquid. In turn, the poor space-filling efficiency of this structure produces a less-organized mesophase. The C_{60} units are not as closely packed as in **2a** and **2b**, and they adopt a more random arrangement, as suggested by the absence of the middle-angle diffuse maximum in the X-ray patterns of **1b**. The (002) reflection is absent in all the X-ray patterns, whereas the (003) reflection is unusually strong. This suggests that the projection of the electron density profile on the direction normal to the layers contains three well-defined maxima with a period of about $d/3$ (d = measured spacing). These electron density maxima correspond to three regions respectively containing the fullerene sublayer and the two sublayers of bent-shaped units. Therefore the distribution of the X-ray intensities, dominated by the contribution of the third-order harmonic, agrees well with the features of the proposed structure.

From the data discussed above it can be stated that, with the exception of compound **1a**, in a subtle balance of intermolecular interactions, increases in temperature help disturb the solid arrangements of these simple nondendritic fullerene monoadducts, but the bent-core structures retain the molecular contacts to form compact lamellar mesophases through the microsegregation of the structural motifs.

This segregated organization arises from a combination of efficient space filling and strong interactions within each microdomain. Regions of C_{60} units are intercalated between regions of well-organized bent-shaped units, which are responsible for the supramolecular layer organization. Nevertheless, the role of the fullerene moiety also seems to be significant in these compounds. Thus, on cooling of the isotropic liquid, **1b** and **2a** slowly self organize, thus discouraging the formation of the liquid-crystal state, while a longer bent-core structure (as in **2b**) appears to lead to a faster soft-matter rearrangement, thus recovering the lamellar liquid-crystalline order. In addition, a comparison of the liquid-crystalline properties of compound **2b** and the malonate **M** (see Ref. [19]) also points to the supramolecular stabilizing role of the fullerene units in this system. The presence of the C_{60} units seems to promote changes in the supramolecular arrangement of the bent-core structures with effects on both the type of molecular packing and the stabilization of the liquid-crystal order. On the other hand, the bulky C_{60} structure also appears to be responsible for the vitrification processes detected in some of these compounds. Interestingly, the hybrid material **2b** forms a glass that retains the order of the previous mesophase at room temperature (glassy mesophase) for very long periods of time through reversible thermal processes, as demonstrated by XRD and MDSC.

An attractive feature of some bent-core liquid-crystalline phases is their switching response under electric fields. This behavior was investigated for these compounds in $5\ \mu\text{m}$ indium tin oxide (ITO) coated cells (see the Supporting Information). The application of a triangular-wave field led to a switching current response without a clear texture change for **2b** (Figure 4). This polarization current, which to our

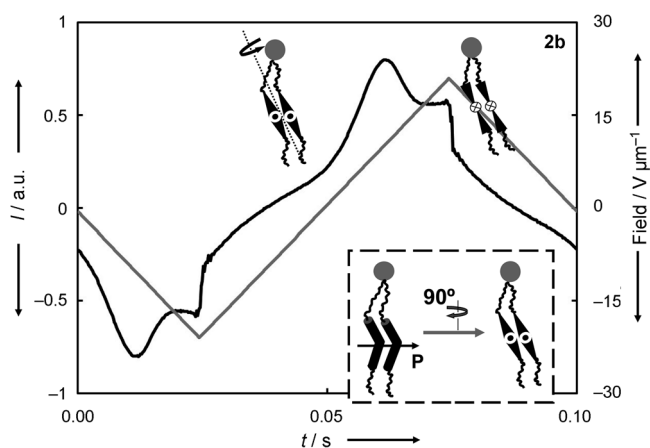


Figure 4. Bottom: Typical schematic representations of bent-core molecules. Top: Polarization switching current in the lamellar polar phase of compound **2b** at $135\ ^\circ\text{C}$, under a triangular-wave electric field: $10\ \text{Hz}$, $42\ \text{Vpp}\ \mu\text{m}^{-1}$. The molecular switching under an electric field in the mesophase is also proposed.

knowledge has not been reported previously for a mesomorphic C_{60} -containing compound, confirms the polar character of the mesophase. The increase of the dielectric permittivity at the isotropic-to-mesophase transition is another sign of the polar order in the materials (see the Supporting Information, Figures S8 and S9). This increase is due to the appearance of a low-frequency mode that should be related to a collective motion of the molecules in the smectic layers possessing polar order.

Based on electrooptic and dielectric results, the response can be attributed to the bent-core switching around the molecular long axis rather than an azimuthal rotation from an antiferroelectric ground state. Spontaneous polarization values of around $60\ \text{nCcm}^{-2}$ were measured for **2b** and, interestingly, preliminary studies on this switched sample showed second harmonic generation (SHG) activity at room temperature and in the absence of an electric field.^[20] Unfortunately this kind of study could not be carried out on compounds **1b** and **2a** because the high temperature transitions prevented the preparation of suitable cells for **1b**, and owing to the dielectric breakdown of the cells in the case of **2a**. A study of the dielectric behavior of **2a** and **2b** confirmed the presence of a mesophase in both compounds (see the Supporting Information).

In summary, we have prepared innovative nondendritic hybrid C_{60} -containing bent-core molecules that form lamellar organizations. The potential of [60]fullerene units in an ordered and easily processed soft phase could be combined with organic functional moieties and the unique bent-core liquid-crystal properties, such as supramolecular chirality, optoelectronic features, and polar order. The temperature range of the mesophase, the nanosegregation of the C_{60} units, the stabilization of the soft supramolecular order even at room temperature, and the molecular responses to external stimuli, such as electric fields, for these C_{60} -containing bent-core molecules, all depend on the molecular structure and can be modified by changing the molecular design. Furthermore, the dielectric response of these materials, as well as their

redox properties, confirm that this new type of C₆₀-based liquid crystal represents an advantageous strategy for the design of new functional systems.

Received: July 12, 2011

Published online: November 4, 2011

Keywords: fullerenes · liquid crystals · molecular electronics · organic functional materials · supramolecular chemistry

- [1] Special features on molecular electronics: C. Joachim, M. A. Ratner, *Proc. Natl. Acad. Sci. USA* **2005**, *102*, 8800 and related papers in this issue; *Chem. Rev.* **2010**, *110*, 1–574.
- [2] a) N. Martín, L. Sanchez, B. Illescas, I. Perez, *Chem. Rev.* **1998**, *98*, 2527–2548; b) L. Echegoyen, L. E. Echegoyen in *The Electrochemistry of C₆₀ and Related Compounds* (Eds.: L. Henning, O. Hammerich), Marcel Dekker, New York, **2001**; c) D. Gust, T. A. Moore, A. L. Moore, *Acc. Chem. Res.* **2001**, *34*, 40–48; d) D. M. Guldi, *Chem. Soc. Rev.* **2002**, *31*, 22–36; e) H. Imahori, *J. Phys. Chem. B* **2004**, *108*, 6130–6143; f) H. Imahori, *Org. Biomol. Chem.* **2004**, *2*, 1425; g) J. L. Segura, N. Martín, D. M. Guldi, *Chem. Soc. Rev.* **2005**, *34*, 31–47; h) F. Langa, J. F. Nierengarten, *Fullerene Principles and Applications*, RSC Publishing, London, **2007**; i) “Carbon Nanotubes and Related Structures: Synthesis Characterization, Functionalization, and Applications” (Eds.: D. M. Guldi, N. Martín), Wiley-VCH, Weinheim, **2010**.
- [3] a) S. R. Wilson, D. L. Schuster, B. Nuber, M. S. Meier, M. Maggini, M. Prato, R. Taylor in *Organic Chemistry of Fullerenes* (Eds.: K. M. Kadish, R. S. Ruoff), Wiley Interscience, New York, **2000**; b) A. Hirsch, M. Brettreich in *Fullerenes: Chemistry and Reactions*, Wiley-VCH, Weinheim, **2004**; c) N. Martín, *Chem. Commun.* **2006**, 2093–2104.
- [4] a) L. Sánchez, N. Martín, D. M. Guldi, *Angew. Chem.* **2005**, *117*, 5508–5516; *Angew. Chem. Int. Ed.* **2005**, *44*, 5374–5382; b) E. M. Pérez, N. Martín, *Chem. Soc. Rev.* **2008**, *37*, 1512–1519; c) T. Nakanishi, *Chem. Commun.* **2010**, *46*, 3425–3436; d) S. S. Babu, H. Möhwald, T. Nakanishi, *Chem. Soc. Rev.* **2010**, *39*, 4021–4035; e) D. Canevet, E. Pérez, N. Martín, *Angew. Chem.* **2011**, *123*, 9416–9427; *Angew. Chem. Int. Ed.* **2011**, *50*, 9248–9259.
- [5] a) S. Campidelli, C. Eng, M. I. Saez, J. W. Goodby, R. Deschenaux, *Chem. Commun.* **2003**, 1520–1521; b) S. Campidelli, J. Lenoble, J. Barberá, F. Paolucci, M. Marcaccio, D. Paolucci, R. Deschenaux, *Macromolecules* **2005**, *38*, 7915–7925; c) H. Mamlouk, B. Heinrich, C. Bourgoigne, B. Donnio, D. Guillon, D. Felder-Flesch, *J. Mater. Chem.* **2007**, *17*, 2199–2205; d) N. Maringa, J. Lenoble, B. Donnio, D. Guillon, R. Deschenaux, *J. Mater. Chem.* **2008**, *18*, 1524–1534; e) S. Campidelli, P. Bourgun, B. Guintchin, J. Furrer, H. Stoeckli-Evans, I. M. Saez, J. W. Goodby, R. Deschenaux, *J. Am. Chem. Soc.* **2010**, *132*, 3574–3581; f) S. Campidelli, L. Pérez, J. Rodríguez-López, J. Barberá, F. Langa, R. Deschenaux, *Tetrahedron* **2006**, *62*, 2115–2122; g) L. Pérez, J. Lenoble, J. Barberá, P. De La Cruz, R. Deschenaux, F. Langa, *Chem. Commun.* **2008**, 4590–4592.
- [6] a) M. Sawamura, K. Hawaii, Y. Matsuo, K. Kanie, T. Kato, E. Nakamura, *Nature* **2002**, *419*, 702–705; b) Y. Matsuo, A. Muramatsu, Y. Kamikawa, T. Kato, E. Nakamura, *J. Am. Chem. Soc.* **2006**, *128*, 9586–9587; c) S. Campidelli, T. Brandmuller, A. Hirsch, I. M. Saez, J. W. Goodby, R. Deschenaux, *Chem. Commun.* **2006**, 4282–4284; d) J. Lenoble, N. Maringa, S. Campidelli, B. Donnio, D. Guillon, R. Deschenaux, *Org. Lett.* **2006**, *8*, 1851–1854; e) Y. W. Zhong, Y. Matsuo, E. Nakamura, *J. Am. Chem. Soc.* **2007**, *129*, 3052–3053.
- [7] a) T. Chuard, R. Deschenaux, *J. Mater. Chem.* **2002**, *12*, 1944–1951; b) B. Dardel, D. Guillon, B. Heinrich, R. Deschenaux, *J. Mater. Chem.* **2001**, *11*, 2814–2831.
- [8] a) T. Nakanishi, Y. Shen, J. Wang, S. Yagai, M. Funahashi, T. Kato, P. Fernández, H. Möhwald, D. G. Kurth, *J. Am. Chem. Soc.* **2008**, *130*, 9236–9237; b) P. A. L. Fernandes, S. Yagai, H. Möhwald, T. Nakanishi, *Langmuir* **2010**, *26*, 4339–4335; c) S. Orlandi, L. Muccioli, M. Ricci, C. Zannoni, *Soft Mater.* **2009**, *5*, 4484–4491.
- [9] a) G. Pelzl, S. Diele, W. Weissflog, *Adv. Mater.* **1999**, *11*, 707; b) C. Tschierske, G. Dantlgraber, *Pramana. J. Phys.* **2003**, *61*, 455–481; c) D. M. Walba, *Top. Stereochem.* **2003**, *24*, 457–476; d) M. B. Ros, J. L. Serrano, M. R. De La Fuente, C. L. Folcia, *J. Mater. Chem.* **2005**, *15*, 5093–5098; e) R. Amarantha Reddy, C. Tschierske, *J. Mater. Chem.* **2006**, *16*, 907–961; f) H. Takezoe, Y. Takahashi, *Jpn. J. Appl. Phys.* **2006**, *45*, 597–625; g) W. Weissflog, H. N. Sheenivasa Murthy, S. Diele, G. Pelzl, *Philos. Trans. R. Soc. London Ser. A* **2006**, *364*, 2657–2679; h) G. Pelzl, W. Weissflog in *Thermotropic liquid crystals, Recent advances* (Ed.: A. Ramamoorthy), Springer, Dordrecht, **2007**, chap. 1.
- [10] a) A. Jákli, C. Bailey, J. Harden in *Thermotropic liquid crystals, Recent advances* (Ed.: A. Ramamoorthy), Springer, Dordrecht, **2007**, chap. 2; b) J. Etxebarria, M. B. Ros, *J. Mater. Chem.* **2008**, *18*, 2919–2926; c) A. Jákli, I. Pintre, J. L. Serrano, M. B. Ros, M. R. De La Fuente, *Adv. Mater.* **2009**, *21*, 3784–3788; d) I. C. Pintre, J. L. Serrano, M. B. Ros, J. Martínez-Perdiguero, I. Alonso, J. Ortega, C. L. Folcia, J. Etxebarria, R. Alicante, B. Villacampa, *J. Mater. Chem.* **2010**, *20*, 2965–2971.
- [11] a) M. Maggini, G. Scorrano, M. Prato, *J. Am. Chem. Soc.* **1993**, *115*, 9798–9799; b) N. Tagmatarchis, M. Prato, *Synlett* **2003**, 768–779; c) N. Martín, M. Altabe, S. Filippone, A. Martín-Domenech, L. Echegoyen, C. M. Cardona, *Angew. Chem.* **2006**, *118*, 116–120; *Angew. Chem. Int. Ed.* **2006**, *45*, 110–114.
- [12] a) D. Shen, A. Pegenau, S. Diele, I. Wirth, C. Tschierske, *J. Am. Chem. Soc.* **2000**, *122*, 1593–1601; b) N. Gimeno, M. B. Ros, J. L. Serrano, R. De La Fuente, *Angew. Chem.* **2004**, *116*, 5347–5350; *Angew. Chem. Int. Ed.* **2004**, *43*, 5235–5238; c) J. Barberá, N. Gimeno, L. Monreal, R. Pinol, M. R. Ros, J. L. Serrano, *J. Am. Chem. Soc.* **2004**, *126*, 7190–7191.
- [13] a) C. Bingel, *Chem. Ber.* **1993**, *126*, 1957–1959; b) X. Camps, A. Hirsch, *J. Chem. Soc. Perkin Trans. 1* **1997**, 1595–1596.
- [14] Although Bingel cycloadducts can undergo a retro-cyclopropanation reaction (retro-Bingel reaction) under electrochemical and chemical reduction conditions, those processes occur under specific experimental conditions (controlled potential electrolysis). In our case, and under the CV experimental conditions, the observed waves can be reasonably assigned to the reduction processes occurring on the fullerene unit. For more details, see: a) R. Kessinger, J. Crassous, A. Herrmann, M. Ruttimann, L. Echegoyen, F. Diederich, *Angew. Chem.* **1998**, *110*, 2022–2025; *Angew. Chem. Int. Ed.* **1998**, *37*, 1919–1922; b) R. Kessinger, N. S. Fender, L. E. Echegoyen, C. Thilgen, L. Echegoyen, F. Diederich, *Chem. Eur. J.* **2000**, *6*, 2184–2192; c) M. W. J. Beulen, L. Echegoyen, J. A. Rivera, M. A. Herranz, A. Martín-Domenech, N. Martín, *Chem. Commun.* **2000**, 917–918; d) M. W. J. Beulen, J. A. Rivera, M. A. Herranz, A. Martín-Domenech, N. Martín, L. Echegoyen, *Chem. Commun.* **2001**, 407–408; e) M. W. J. Beulen, J. A. Rivera, M. A. Herranz, B. Illescas, N. Martín, L. Echegoyen, *J. Org. Chem.* **2001**, *66*, 4393–4398; f) M. A. Herranz, M. W. J. Beulen, J. A. Rivera, L. Echegoyen, M. C. Díaz, B. M. Illescas, N. Martín, *J. Mater. Chem.* **2002**, *12*, 2048–2053.
- [15] For details about the MDSC technique and its application to liquid-crystal materials see: a) M. B. Sied, J. Salud, D. O. López, M. Barrio, J. L. Tamarit, *Phys. Chem. Chem. Phys.* **2002**, *4*, 2587–2593; b) N. Sebastián, M. R. de La Fuente, D. O. López, M. A.

Pérez-Jubindo, J. Salud, S. Diez-Berart, M. B. Ros, *J. Phys. Chem. B* **2011**, *115*, 9766–9775.

- [16] a) D. Felder-Flesch, L. Rupnicki, C. Bourgoigne, B. Donnio, D. Guillon, *J. Mater. Chem.* **2006**, *16*, 304–309; b) J. Wang, Y. Shen, S. Kessel, P. Fernandes, Y. Kaname, Y. Shiki, D. G. Kurth, H. Möhwald, T. Takahashi, *Angew. Chem.* **2009**, *121*, 2200–2204; *Angew. Chem. Int. Ed.* **2009**, *48*, 2166–2170.
- [17] Further studies on the aligned samples should enable the determination of the tilted (SmCP) or nontilted (SmAP) structure of these materials (L. Guo et al., *Soft. Mater.* **2011**, *7*, 2895–2899; R. A. Reddy, *Science* **2011**, *332*, 72–77).
- [18] The cross-sectional area is 90–100 Å² for C₆₀ and 22–25 Å² for classical rod-like units. The cross-section of a bent-core molecule is larger and tilting also increases this area.
- [19] The dimer **M** exhibits a narrow liquid-crystal phase on heating, as deduced from DSC, MDSC, and dielectric studies (Table 1, Figure 1 and see the Supporting Information). This mesophase is consistent with a columnar order according to the optical texture; unfortunately, crystallization prevented further characterization by XRD.
- [20] SHG activity of the sample cell (5 μm thick) was surveyed at room temperature, as a fingerprint indication of polar order (noncentrosymmetric arrangement). A very weak signal at 953 nm was detected when rotating the cell around a vertical axis, perpendicular to the incidence plane of the 1907 nm excitation light. However, it must be noted that proper characterization of the *d_{ij}* coefficients of these materials requires well-aligned samples (J. Ortega, J. A. Gallastegui, C. L. Folcia, J. Etxebarria, N. Gimeno, M. B. Ros, *Liq. Cryst.* **2004**, *31*, 579–584) and more precise measurements will be performed as part of a future project.